Water, proton, and oxygen transport in high IEC, short side chain PFSA ionomer membranes: consequences of a frustrated network

Luo, Xiaoyan; Holdcroft, Steven; Mani, Ana; Zhang, Yongming; Shi, Zhiqing

Publisher's version / Version de l'éditeur:
https://doi.org/10.1039/c1cp22559f
Physical Chemistry Chemical Physics, 13, 40, pp. 18055-18062, 2011-09-13

PCCP

Cite this: *Phys. Chem. Chem. Phys.*, 2011, **13**, 18055–18062

www.rsc.org/pccp

PAPER

Water, proton, and oxygen transport in high IEC, short side chain PFSA ionomer membranes: consequences of a frustrated network†

Xiaoyan Luo,[a] Steven Holdcroft,*[ac] Ana Mani,[a] Yongming Zhang[b] and Zhiqing Shi[c]

Received 8th August 2011, Accepted 24th August 2011
DOI: 10.1039/c1cp22559f

The effect of ion exchange capacity (IEC) on the water sorption properties of high IEC, short side chain (SSC) PFSA ionomer membranes, and the relationships between water content, proton conductivity, proton mobility, water permeation, oxygen diffusion, and oxygen permeation are investigated. SSC PFSA ionomer membranes possessing 1.3, 1.4, and 1.5 mmol g^{-1} IEC are compared to a series of long side chain (LSC) PFSA ionomer membranes ranging in IEC from 0.9 to 1.13 mmol g^{-1}. At 25 °C, fully-hydrated SSC ionomer membranes are characterized as possessing higher water contents (56–75 vol%), moderate λ values (15–18), high analytical acid concentrations (2–2.8 M), and moderate conductivity (88–115 mS/cm); but lower than anticipated effective proton mobility. Complementary measurements of water permeability, oxygen diffusion, and oxygen permeability also yield lower than expected values given their much higher water contents. Potential benefits afforded by reducing the side chain length of PFSA ionomer membranes, such as increased crystallinity, higher IEC, and high hydrated acid concentration are offset by a less-developed, frustrated hydrophilic percolation network, which provides a motivation for future improvements of transport properties for this class of material.

Introduction

Perfluorosulfonic acid (PFSA) ionomer is the preferred material for use in membranes for current generation PEM fuel cells. For several decades Nafion®, commercialized by the E.I. Dupont Co. has been the benchmark PFSA ionomer membrane for low–to-medium temperature PEMFCs. Significant attention has been paid to reducing the thickness and improving its chemical stability.[1] Nafion® possesses many desirable properties for PEMFC applications but still suffers from poor proton conductivity under low relative humidities. Nafion PFSA membrane is a long-side-chain (LSC) ionomer (Scheme 1a). A promising derivative utilizes a short-side-chain (SSC) ionomer (Scheme 1b). This class of polymer was originally introduced by the Dow Chemical Co. in the 1980s but commercially abandoned because of its complicated synthesis and high cost; despite the improvements observed in fuel cell performance over LSC ionomer memebranes.[2] Recently, a simpler synthetic route to the SSC ionomer was developed by Solvay Solexis. Membranes under the trade name, Aquivion® -previously Hyflon® ion, possess similar properties to the original Dow ionomer membranes,[3] and compared to LSC analogues exhibit a higher degree of crystallinity, enhanced proton conductivity and higher Tg,[4] which collectively confer improved mechanical durability, greater fuel cell efficiency, and enable higher temperature operation. An increasing number of studies describing the properties of SSC PFSA ionomer membranes are reported.[4–8] Kreuer and co-workers[9] studied Dow 840 (840 g mol^{-1}) and Dow 1150, reporting that SSC PFSA membranes displayed similar water and proton transport and similar hydrophobic/hydrophilic separation as a

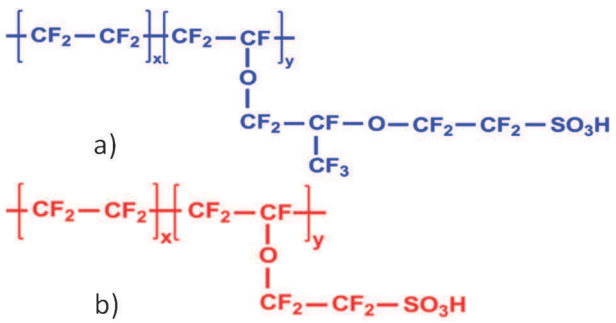

Scheme 1 PFSA ionomers: (a) long side chain (LSC); (b) short side chain (SSC).

[a] *Department of Chemistry, Simon Fraser University, 8888 University Drive, Burnaby, British Columbia, Canada V5A 1S6. E-mail: holdcrof@sfu.ca; Fax: +1(778) 782-3785; Tel: +1 (778) 782 4221*
[b] *School of Chemistry and Chemical Technology, Shanghai Jiao Tong University, 800 Dongchuan Road, Shanghai 200240, China*
[c] *Institute for Fuel Cell Innovation, National Research Council Canada, Vancouver, British Columbia, Canada V6T 1W5*
† Electronic supplementary information (ESI) available. See DOI: 10.1039/c1cp22559f

function of water volume fraction in comparison to Nafion® 117 at a given IEC. The connectivity of the hydrophilic channels was reported to be reduced due to the reduced flexibility of the short side-chain architecture. Gorri *et al.*[10] explored water and methanol permeation through SSC Hyflon® 860 membranes and reported that water and methanol fluxes increase with temperature. De Angelis *et al.* studied the effect of temperature on water sorption and diffusion in a SSC PFSA membrane (EW = 860 g mol^{-1}) and demonstrated that water diffusivity reaches a maximum value when the water content approaches maximum values of hydration of -SO_3H groups.[11] SSC ionomers have also been the subject of several theoretical and molecular-level modelling studies,[12–18] from which, the effect of backbone flexibility, length of side chain, IEC, and molecular weight on proton transport processes, under varying levels of hydration, has been revealed.

Compared to LSC PFSA analogues, the shorter side chain should allow for a much greater IEC without causing excessive swelling or dissolution. This is because the main chain sequence length between side chains will, on average, be longer for a given IEC, and hence the extent of main chain crystallization, potentially greater. However, reported studies of high IEC, SSC PFSA ionomer membranes are relatively few. Moore and Martin[19] studied the Na^+-form of Dow's PFSA ionomer membranes (EW = 635, 803, 909, 1076 and 1269 g mol^{-1}) using WAXS. The analysis revealed that high IEC SSC membranes possessed a lower crystallinity index than low IEC analogues. DSC analysis revealed that Dow 635 membrane possessed endotherms due to a glass transition and a thermal transition involving ionic clusters. Compared to high EW Dow membranes, the 635 EW membrane exhibits a higher ionic cluster glass transition temperature. Also, high IEC membranes absorb more water and possess larger ionic clusters than low IEC membranes. It is also reported that Dow 635 Na^+-form membrane absorbs up to 80% water due to the formation of an interconnected rod-like network.[20] Ghielmi[3] *et al.* examined water uptake of extruded Hyflon 670 (IEC = 1.49 mmol g^{-1}) and 770 (IEC = 1.30 mmol g^{-1}) membranes at 100 °C. Much larger water uptakes were observed compared to low IEC Hyflon membranes, and molecular modelling studies of proton transport in SSC PFSA membranes (IEC = 1.72 mmol g^{-1}) revealed that the calculated hydronium ion diffusion coefficient increased with water content.[18]

Noteworthy, the studies referred to above describe properties of SSC PFSA ionomer membranes prepared by extrusion; the properties of solution-cast SSC PFSA membranes is sparse, despite the significant effect processing conditions exert on membrane properties, as clearly demonstrated for LSC PFSA ionomer membranes.[1] Recently, we reported fuel cell performances of membrane-electrode-assemblies using high IEC SSC ionomer (1.3, 1.4, 1.5 mmol g^{-1}) as the proton conducting medium dispersed in the catalyst layer.[21] The incorporation of high IEC SSC ionomer provided improved fuel cell polarization performance at elevated temperature and under lower relative humidity.

In this report, attention is turned to understanding the physicochemical and transport properties of high IEC SSC ionomer membranes. We examine the effect of IEC on water sorption, proton conductivity, and proton mobility.[22] Due to the anomalous and unpredicted properties observed, molecular transport properties were further examined using: hydraulic permeability, in the case of water transport, according to our previously developed methodology;[23] and electrochemical oxygen reduction in a solid state electrochemical cell, in order to determine oxygen diffusion, solubility and permeability.[24] The properties of SSC membranes are compared to LSC PFSA membranes possessing varying IEC in order that similarities and deviations between the two can be elucidated.

Experimental

Materials

Short side chain (SSC) PFSA membranes (20 μm thick), solution-cast from DMF, and provided by Shandong Dongyue Chemical Co. Ltd, were synthesized using a previously described route from $CF_2CF(OCF_2CF_2SO_2F)$ monomer.[25] SSC PFSA ionomers possessed the following IECs (EW): 1.3 (770), 1.4 (715) and 1.5 mmol g^{-1}(670 g mol^{-1}). These are abbreviated: SSC-1.3, SSC-1.4, and SSC-1.5, respectively.

Long side chain (LSC) PFSA membranes (~19 μm thick) were provided by Shandong Dongyue Chemical Co. Ltd. The membranes were also cast from DMF solutions. LSC PFSA ionomers possessed the following IECs (EW): 0.94(1063), 1.05(954), 1.06(943), 1.09(917), 1.13 mmol g^{-1} (885 g mol^{-1}). These are abbreviated: LSC-0.94, LSC-1.05, LSC-1.06, LSC-1.09, LSC-1.13. Nafion® 211(25 μm thick) was purchased from Aldrich.

Sulfuric acid and sodium chloride (99%, reagent grade) were purchased from Alfa Aesar and used as-received. Hydrogen peroxide and sodium hydroxide were purchased from Sigma Aldrich and used as-received. Milli-Q water (Millipore) (18 mΩ) was used for washing and hydrating membranes.

Membranes were first boiled in 3 vol% H_2O_2 solution for 1 h, and washed with Millipore water for an hour, during which time the water was refreshed several times. Membranes were subsequently boiled in 1 M H_2SO_4 for 1 h. Finally, membranes were boiled in Millipore deionized water for 1 h and washed repeatedly in fresh water until the pH of the water remained constant. Membranes were stored in Millipore deionized water overnight prior to use.

Characterization

Ion exchange capacity (IEC) (mmol g^{-1}) was determined by titration. Samples (~10 × 20 mm) were cut from fully hydrated membranes and equilibrated in 50 ml 2 M NaCl overnight at room temperature prior to use. The protons released were neutralized using a 0.001 M NaOH to a phenolphthalein end point. IEC was calculated according to a standard formula.[26]

Water sorption was determined as water uptake, water volume fraction (X_v), and λ, using eqn (1), (2) and (3), respectively:

$$Water\ uptake = \frac{W_{wet} - W_{dry}}{W_{dry}} \quad (1)$$

$$X_v = \frac{V_{water}}{V_{wet}} \quad (2)$$

$$\lambda = \frac{water\ uptake(\%) \times 10}{18 \times IEC(mmol/g)} \quad (3)$$

where W_{wet} and W_{dry} are the 'wet' and 'dry' weight of the membrane, respectively. 'Wet' membranes were equilibrated in Millipore deionized water overnight at room temperature, removed, and surface water removed. 'Dry' membranes were obtained by placing the membrane under vacuum overnight at 80 °C and cooled in a desiccator. V_{water} is the volume of water contained in the membrane (the water density was taken as 1.0 gcm^{-3}); and V_{wet}, the total volume of the wet membrane. To obtain V_{water}, the mass of free water in the membrane and its density were used. In order to estimate V_{wet}, the membrane dimensions were measured using a digital micrometer (±0.001 mm, Mitutoyo) and digital callipers (±0.1 mm, Mitutoyo).

Polymer dry density was calculated using eqn (4):

$$\rho = \frac{W_{dry}}{V_{wet} - V_{H_2O}} \quad (4)$$

where W_{dry} is the weight of dry sample, V_{wet} is the volume of the wet sample, and V_{H_2O} is the volume of water in the wet membrane.

Proton conductivity was measured using EIS with a Solartron 1260 frequency response analyzer (FRA) within the frequency range of 10 MHz–100 MHz using an in-plane, two-electrode configuration. A strip of fully hydrated membrane was contacted by two Pt electrodes, and a 100 mV sinusoidal AC voltage was passed along the plane of the sample. More details of the experimental procedure can be found in ref. 22. Proton conductivity was calculated using eqn (5):

$$\sigma_{H^+} = \frac{L}{RA} \quad (5)$$

where L (cm) is the distance between electrodes, R (Ω) is the ionic resistance of the membrane and A (cm^2) is the cross sectional area of the sample.

Acid concentration and effective proton mobility was calculated using eqn (6) and (7).

$$[-SO_3H] = \frac{W_{dry}(g)}{V_{wet}(cm^3)} \times IEC(mmol/g) \quad (6)$$

$$\mu'_{H^+} = \frac{\sigma_{H^+}}{F[-SO_3H]} \quad (7)$$

Hydraulic permeability was determined for liquid-equilibrated membranes wherein a pressure gradient of liquid water was forced across the experiment cell. A syringe (Gastight® #1025, Hamilton Co. with PHD2000, Harvard Apparatus) filled with deionized water, a mass flow meter (2.0 μL/min μ-FLOW, Bronkhorst HI-TEC) and a pressure transducer (PX302-100GV, Omega Engineering Inc.) were connected in series with "1/8" OD PTFE tubing. The membrane was placed in a cell consisting of a PTFE coated stainless steel screen and an O-ring. The cell was operated at 24 (±1) °C. Measurements were taken in the constant flow rate mode when the pressure had equilibrated. The apparatus was controlled and monitored using Labview® software. Further details of the measurement are reported elsewhere.[23] For hydraulic permeability measurements only, the thicknesses of the SSC ionomer membranes were >20 μm, and are listed in the results section.

Oxygen solubility, diffusion, and permeability were measured using solid-state electrochemical cell methodology.[27–30] The solid polymer electrolyte membrane was sandwiched between a 50 μm radius Pt micro-disc working electrode (WE), Sandfire Scientific Ltd., Gibsons, Canada, diametrically opposed to a 0.25 mm diam. Pt wire of a dynamic hydrogen electrode (DHE) and a Pt gauze counter electrode (CE). The assembly was housed in a home-built environmental chamber. Prior to electrochemical analysis, the electrodes were polished with 0.05 micron alumina. In order to increase the surface area of the Pt micro-disc, the electrode was platinized by potential cycling (1.2 V to −0.2 V) in 1 mM K_2PtCl_6 in 0.5 M H_2SO_4 solution at 50 mV/s scan rate for ~5 h. The electrochemical response of the working electrode was examined in N_2-saturated 0.5 M H_2SO_4 *versus* a saturated calomel electrode (SCE). The electrochemical surface area (ESA) was estimated using the charge under the hydrogen adsorption region of a voltammogram using 210 μC cm^{-2} as the conversion factor for charge-to-area.[31] The geometric area was 7.854×10^{-5} cm^2 and the roughness factor was 2.5.

Cyclic voltammograms (CVs) were recorded using an EG & G PARC Model 283 potentiostat. The oxygen pressure inside the chamber was 30 psi, the relative humidity (RH) was 100% and the temperature was varied from 30 to 70 °C. The electrode was scanned for 100 cycles between 1.4 and 0.1 V at 100 mV/s to clean the Pt | membrane interface prior to measurements. Chronoamperometry (CA) was carried out by holding the potential of the Pt micro-disc at 1.2 V for 20 s and then stepping to 0.4 V for 10 s. Values of D_{O2}, C_{O2} and P_{O2} were obtained from the average of five chronoamperometric trials according to published procedures.[27,29]

Results and discussion

Water sorption

Water volume content, X_ν, and number of water molecules per sulfonic acid group, λ, of fully hydrated SSC PFSA membranes at ~25 °C are shown in Fig. 1. Notwithstanding the fact that only 3 membranes of different IEC were available for analysis, the water contents are observed to increase with IEC, both in terms of X_ν and λ. X_ν for SSC membranes is 2 to 4 times larger than for LSC membranes which also increases with IEC in accordance to the typical trend observed for LSC PFSA membranes. The water volume contents for the SSC membranes (56 to 75%) are much larger than for N211 (26%).

λ for SSC-1.3 (~15) is similar to that exhibited by LSC membranes that possess much smaller IECs (0.9–1.13 mmol/g) but slightly larger than N211 (~13). The increasing λ with IEC for the SSC membranes falls on a lower trend line than that for LSC membranes, indicating that water sorption is slightly suppressed for a given IEC. SSC membranes exhibit much higher water content, X_ν, than LSC membranes but possess relatively similar λ values – as illustrated in a plot of λ against X_ν (see Supporting Information, Fig. S1†). This is due to the SSC membranes possessing a greater dry polymer density (see Supporting Information Fig. S2†). Plots of λ against X_ν often reveal insights into membrane swelling phenomena: for example, λ may remain unchanged over a wide range of X_ν, increase steadily with X_ν, or may increase dramatically at a given water

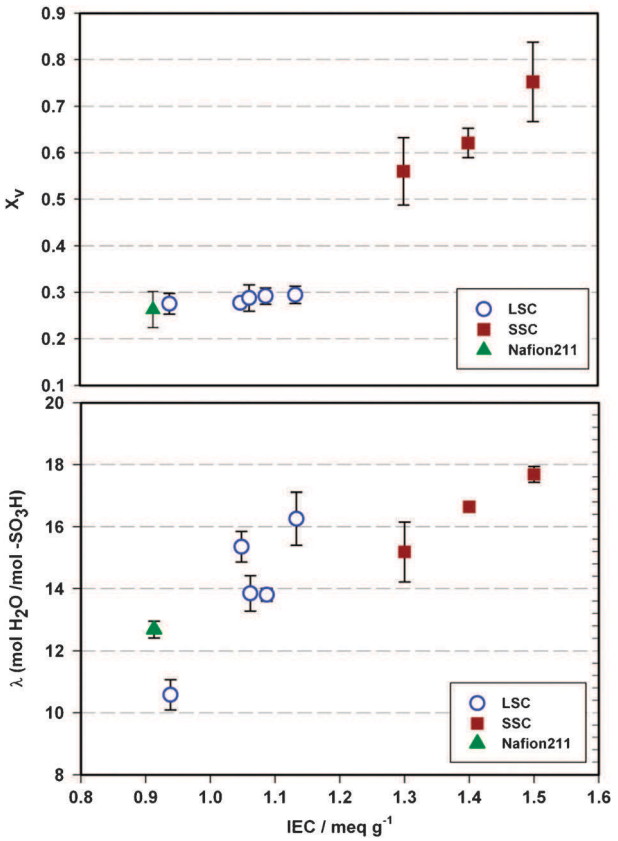

Fig. 1 Water content (X_v and λ) of fully hydrated SSC PFSA, LSC PFSA and Nafion 211membranes, as a function of IEC at ~25 °C.

volume.[22] In the present case, based on the observed trends for SSC and LSC, SSC swells less than LSC for a given IEC.

Proton conductivity and acid concentration

The proton conductivity of the 3 fully-hydrated SSC PFSA membranes at ~25 °C ranged between 88 and 115 mS/cm as shown in Fig. 2. No obvious trend exists between conductivity and IEC within this series. In contrast, the proton conductivity of LSC PFSA membranes increases with increasing IEC, consistent with reports for Nafion-based membranes. A commercial sample of N211 falls on the trend line for the LSC membranes. The SSC PFSA membranes exhibit higher conductivity than N211 and exhibit similar values to LSC membranes having IECs 0.9 to 1.13 mmol g^{-1}. However, it is clear the SSC membranes do not scale in proton conductivity as a function of IEC according to the trend observed for the LSC membranes—that is, the SSC membranes possessed much lower proton conductivity than anticipated, given their high IEC.

It is pertinent to investigate the relationship between conductivity and water content because hydrated protons travel through the aqueous phase of the ionomer membrane. A plot of conductivity as a function of water content (X_v) is plotted in Fig. 3. A remarkable feature is that despite the water contents (X_v) of SSC membranes being 2 to 2.5 times larger than LSC membranes, and despite proton conduction being very dependent on water volume—as illustrated by the large increase in conductivity with small changes in water contents for the LSC membranes series—the SSC membranes only exhibit

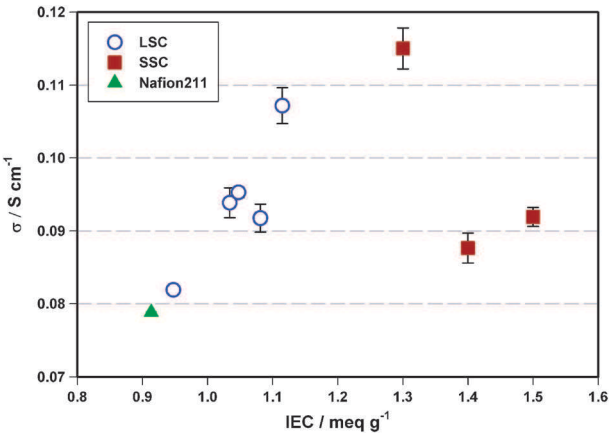

Fig. 2 Proton conductivity of fully hydrated SSC PFSA, LSC PFSA and Nafion 211 membranes as a function of IEC at ~25 °C.

conductivities similar to the highest IEC LSC membranes. Often, high IEC membranes possess low proton conductivities due to excessive sorption of water and reduced proton concentration. However, as illustrated in Fig. 4, the analytical acid concentrations [$-SO_3H$] are ~ twice as large for SSC membranes (2–3 M) as they are for the LSC analogues (1–1.5 M). Thus, as shown in Fig. 4, not only is the water volume in SSC membranes twice as large as in LSC membranes, so too is [$-SO_3H$]. Collectively, these two parameters should impart much higher proton conductivity to the SSC membranes than is observed. This observation is consistent with a report by Kreuer *et al.*[9] that states there is less pronounced separation of hydrophilic and hydrophobic domains in Dow SSC PFSA membranes, resulting in a lower than anticipated proton conductivity.

Effective proton mobility

From measured proton conductivities and calculated values of [$-SO_3H$], the effective proton mobility, μ'_{H+}, was estimated, which provides information on the combined influence of the tortuosity of the hydrophilic pathways and dissociation of the proton and pendent sulfonate anion. Both are strongly influenced by water content. Plots of μ'_{H+} *vs.* X_v and *vs.* IEC are shown in Fig. 5 and a plot of μ'_{H+} *vs.* λ is shown in the

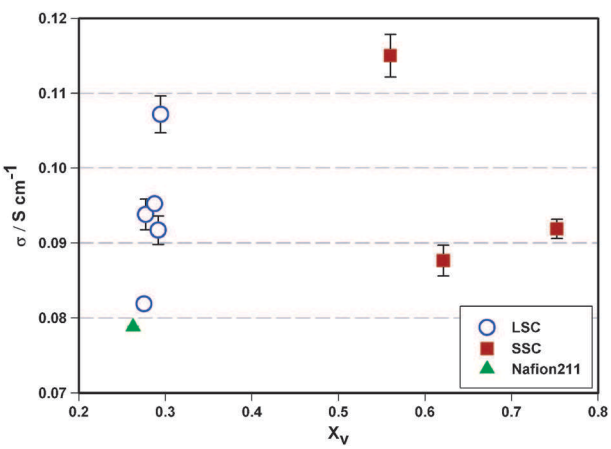

Fig. 3 Proton conductivity of fully-hydrated PFSA membranes as a function of X_v at 25 °C.

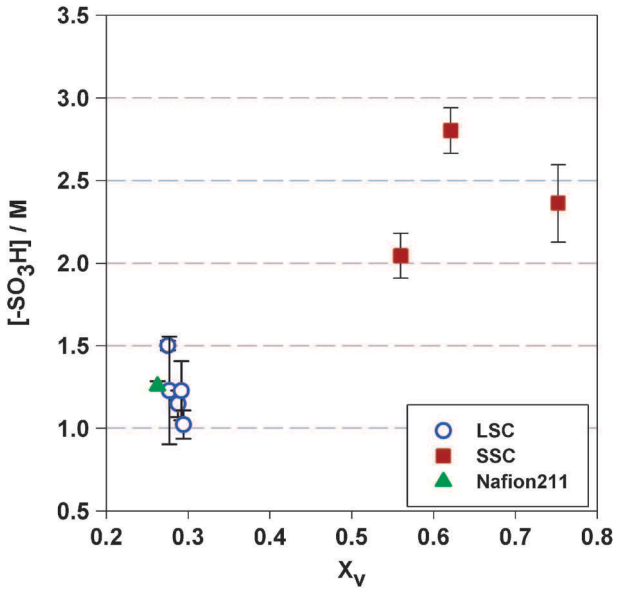

Fig. 4 [$-SO_3H$] of fully hydrated PFSA membranes as a function of X_v at ~25 °C

Supporting Information, Fig. S3.† The proton mobility in SSC membranes is similar in range to N211, even though SSC membranes contain much more water (56–75 vol% compared to ~25 vol% for N211). λ values are similar (SSC ~15, N211 ~13). Moreover, the proton mobilities are much lower than the highest IEC LSC membranes despite the fact that SSC membranes exhibit relatively similar λ values and much higher water contents. Thus proton mobility in SSC membranes is observed to be much lower than expected compared to LSC membranes despite the larger fraction of hydrophilic domains that SSC membranes possess. In relation to this, theoretical modelling indicates that the minimum number of water molecules required to effect proton transfer *increases* with an increase in the number of tetrafluoroethylene (TFE) units in the backbone that separate two juxtapositioned side chains.[32] In the case of SSC ionomer, for a given IEC there are more TFE units that separate the nearest two side chains than in the case of LSC ionomer. Thus a higher water content ($> \lambda$) is needed to effect proton transport in SSC membranes. Our experimental data (shown in Fig. 1) reveal that SSC membranes do not possess much higher λ values than LSC analogues, even though IECs are higher, thus proton mobilities are lower than anticipated, which is consistent with the prediction made through modelling studies.

Water permeation

Water transport through selected membranes was measured under the influence of hydraulic pressure. Water permeation using liquid–liquid interfaces rather than other methods available, such as vapour–vapour permeation (VVP) and liquid–vapour permeation (LVP), was chosen because liquid–liquid interfaces reduce the influence of water vapour adsorption and desorption processes on the overall permeation of water. Thus, hydraulic permeability provides direct information on the mobility of water *within* the membrane, and circumvents complications caused by interfacial water transport.[23]

The hydraulic fluxes of water through SSC membranes are shown in Fig. 6. Each data point represents the steady state flux at a given pressure difference. The slope of the plot, the permeance, decreases in gradient across the series SSC-1.3 to SSC-1.4 to SSC-1.5. Water permeances, and values normalized to membrane thickness, the permeability, are summarized in Table 1.

As can be seen in Table 1, the permeance value for SSC-1.3 (1.42×10^{-13} mPa^{-1} s^{-1}) is ~1/2 that of NR-211 (3.2×10^{-13} mPa^{-1} s^{-1}). The permeance values of SSC-1.4 (1.07×10^{-13} mPa^{-1} s^{-1}) and SSC-1.5 (3.56×10^{-14} mPa^{-1} s^{-1}) are even lower than this. Moreover, much higher pressures were required to achieve the desired flow rate in SSC-1.5. However, hydraulic permeance is thickness dependent and therefore a more meaningful comparison is to normalize these values to thickness to yield permeability data. The permeability of the SSC membranes decreases with IEC. The permeability of SSC-1.5 is almost an order of magnitude smaller than SSC-1.3 and SSC-1.4. The permeabilities of SSC-1.3 (2.28×10^{-17} m^2Pa^{-1} s^{-1}) and SSC-1.4 (2.08×10^{-17} m^2Pa^{-1} s^{-1}), are larger than N211 but not as large as expected given their high water content. Moreover, the permeability of the SSC-1.5 membrane (3.5×10^{-18} m^2Pa^{-1} s^{-1}) is less than half that of N211 (8.0×10^{-18} m^2Pa^{-1} s^{-1}), even though the water content of SSC- 1.5 is ~3 times greater than N211 (75 vol%, *vs.* 26 vol%). The permeabilities of the LSC membranes are much larger than for the SSC membranes. For example, the permeability of LSC- 1.13 (5.31×10^{-15} m^2Pa^{-1} s^{-1}) is ~265 to 1500 times greater than for the SSC membranes, even though its water content is much lower (26 vol%). As in the case of the effective proton mobility the transport of water through SSC membranes is much slower than anticipated given their higher water contents.

As hydrated protons similarly require an aqueous phase for transportation, it was useful to plot the effective proton mobility, μ'_{H+}, versus water permeability, shown in Fig. 7. The effective proton mobility shows a strong correlation with the measured water permeability which confirms the supposition that water and protons travel the same tortuous path.

Oxygen diffusion

Mass transport parameters associated with the oxygen reduction reaction, *i.e.*, O_2 diffusion coefficient, solubility and permeability in one of the SSC membranes (SSC-1.3) was determined chronoamperometrically using a solid state electrochemical cell, as described in the experimental section. In order to aid comparison with the transport properties of protons and water described above, measurements were made at a similar temperature (30 °C). The diffusion coefficient, D_{O2}, solubility, C_{O2} and the product, permeability, P_{O2}, for SSC-1.3 and N211 membranes at are listed in Table 2.

As shown in Table 2, SSC-1.3 membranes exhibit higher D_{O2}, C_{O2} and P_{O2} values compared to N211. Similar to the observations of proton and water transport in SSC-1.3 membranes, this is not an entirely expected result, given that D_{O2}, and P_{O2} are strongly correlated to water content, and C_{O2} inversely correlated.[24,33] The diffusion coefficient and permeability in the SSC-1.3 membrane are lower than anticipated

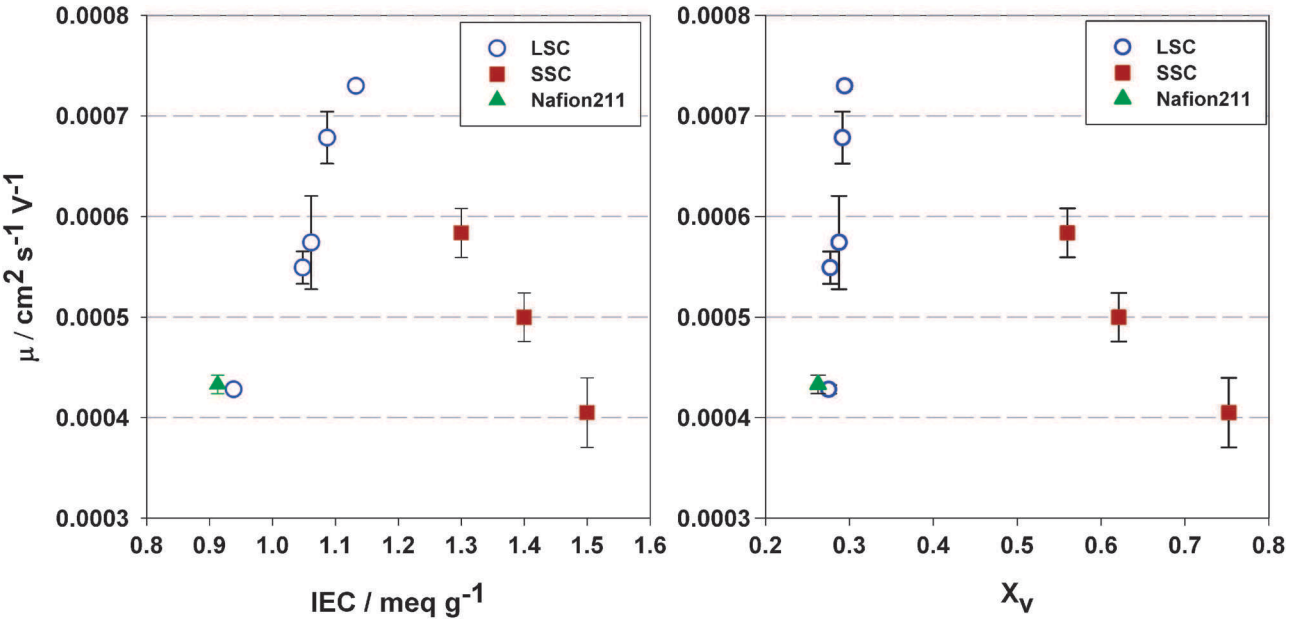

Fig. 5 Effective proton mobility, calculated according to eqn (7), for PFSA ionomer membranes.

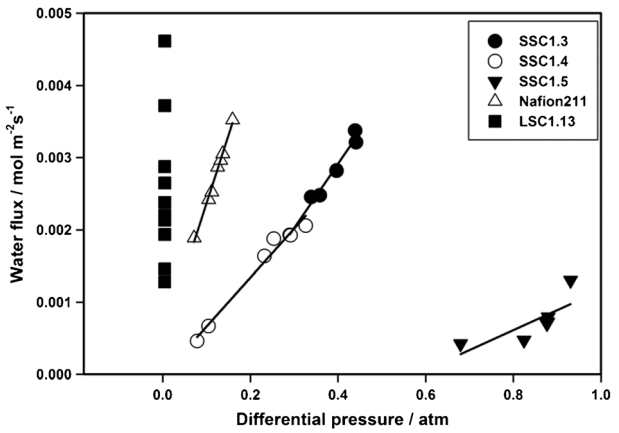

Fig. 6 Water permeation through PFSA PEM as a function of differential hydraulic pressure at ~25 °C.

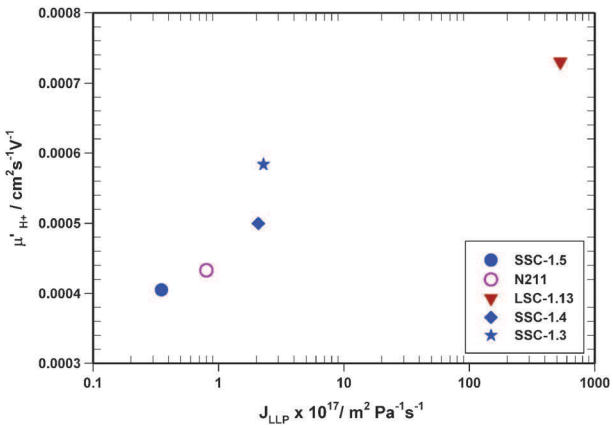

Fig. 7 Effective proton mobility in PFSA ionomer membrane *vs.* water permeability.

Table 1 Hydraulic permeance and permeability of SSC PFSA, LSC PFSA membranes and N211 at ~25 °C

PEM	Thickness (μm)	Water Content (Vol%)	Permeance (mPa^{-1} s^{-1})	Permeability (m^2Pa^{-1} s^{-1})
SSC-1.3	160	56	1.42E-13	2.28E-17
SSC-1.4	195	62	1.07E-13	2.08E-17
SSC-1.5	98	75	3.56E-14	3.50E-18
N211	25	26	3.2E-13	8.00E-18
LSC-1.13	28	29	1.91E-10	5.31E-15

given its much higher water content (56% *vs.* 26 vol%), and the solubility of oxygen is also higher than expected. In the case of previous studies of ORR mass transport parameters determined for other polymer membranes containing more than 50 vol% water, including sulfonated, trifluorostyrenes, block copolymers, and various graft copolymers, under similar conditions, the measured diffusion coefficients and permeabilities are an order of magnitude greater, commensurate with their water content.[34,35]

The observation that proton mobility, water permeance, *and* oxygen diffusion coefficient are all lower in value than anticipated leads us to the conclusions that hydrophilic percolation network for the transport of molecular species is much less developed in SSC membranes than it is for LSC membranes, as originally indicated by Kreuer *et al.*, albeit for an alternate source of SSC PFSA ionomer membrane.[9]

Table 2 ORR mass-transport parameters for SSC 1.3 and Nafion®211 at 30 °C, 100% RH and 30 psi O_2

PEM	$D_{O2} \times 10^6$ (cm^2 s^{-1})	$C_{O2} \times 10^5$ (mol cm^{-3})	$P_{O2} \times 10^{11}$ (mol cm^{-1} s^{-1})
SSC-1.3	1.69 ± 0.42	1.31 ± 0.19	2.22 ± 0.55
Nafion®211	1.13 ± 0.31	1.16 ± 0.17	1.28 ± 0.89

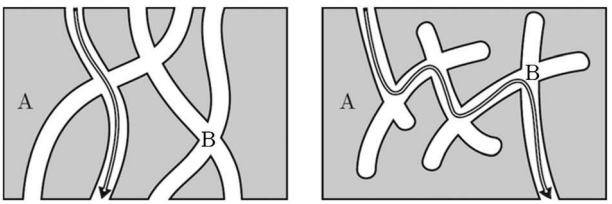

Fig. 8 Schematic diagram illustrating the difference in proton conduction pathways for LSC PFSA (left) and SSC PFSA (right) ionomer membranes, where A represents the perfluorinated matrix; and B, the hydrophilic channels.

Conclusion

In comparison to long side chain PFSA ionomer membranes the SSC membranes studied possessed a higher average IEC and, as a consequence, a much higher water content. The proton conductivity of high IEC, SSC PFSA membranes is greater than N211 membranes, and comparable to the highest IEC LSC membranes examined. The dry polymer density of high IEC SSC membrane was greater than the other membranes examined, the analytical $-SO_3H$ concentration of hydrated membranes was very much higher, but the proton mobility was not as commensurately high, over the range of IEC studied.

While the water uptakes of LSC PFSA ionomer membranes correlate well with the IEC, and the water contents of SSC membranes were commensurately larger due to their much higher IEC, the λ values were lower than expected given the trend observed for LSC membranes. The SSC membranes possessed very high acid concentrations and much higher water contents in comparison to the LSC membranes examined, including Nafion® 211. However, this did not translate into a multi-fold increase in proton conductivity. Rather, SSC membranes were found to possess suppressed proton mobility, even though λ values were reasonably large and the water content very high. This work suggests the network of hydrophilic channels is poorly developed compared to LSC analogues. *Ex-situ* measurements of water permeability and oxygen diffusion, both requiring hydrophilic channels, also support the assertion that the connectivity of the hydrophilic network is not as well developed as in LSC PFSA membranes, suggesting that the additional water volume sorbed into the high IEC SSC membranes is not fully utilized. These observations bring to mind the morphological picture of a larger than usual number of 'dead-ends' or "necking" of channels, as illustrated in Fig. 8, akin to Kreuer's much referenced description of the morphology of hydrocarbon membranes[22] and reiterated for Dow membranes.[9]

This work provides experimental verification of the studies of Brandell *et al.*[17,36] using molecular dynamics studies to assert that SSC-based membranes exhibit a less than ideal connectivity of water channels compared to LSC PFSA ionomer analogues, such as Nafion®. This is in a good agreement with the theoretical studies of Dorenbos *et al.*[37,38] Our study suggests that should the connectivity of the hydrophilic network be improved, and tortuosity reduced, either by finer control of the ionomer structure or by adopting more favourable membrane processing conditions, then the transport properties may be dramatically improved, and proton conductivities increased compared to current SSC PFSA ionomer membranes.

Acknowledgements

The authors would like to thank Shandong Dongyue Chemical Co. Ltd. for synthesis of the SSC and LSC-PFSA ionomers. We also thank the BC Innovation Council and the Natural Sciences and Engineering Research Council of Canada for financial support, Dr Tim Peckham for useful discussions, and Mr Thomas Weissbach for assistance with graphical illustrations.

Notes and references

1 J. Peron, A. Mani, X. Zhao, D. Edwards, M. Adachi, T. Soboleva, Z. Shi, Z. Xie, T. Navessin and S. Holdcroft, *J. Membr. Sci.*, 2010, **356**, 44–51.
2 C. A. Edmondson, P. E. Stallworth, M. E. Chapman, J. J. Fontanella, M. C. Wintersgill, S. H. Chung and S. G. Greenbaum, *Solid State Ionics*, 2000, **135**, 419–423.
3 A. Ghielmi, P. Vaccarono, C. Troglia and V. Arcella, *J. Power Sources*, 2005, **145**, 108–115.
4 M. Gebert, A. Ghielmi, L. Merlo, M. Corasaniti and V. Arcella, *ECS Trans.*, 2010, **26**, 279–283.
5 V. Arcella, C. Troglia and A. Ghielmi, *Ind. Eng. Chem. Res.*, 2005, **44**, 7646–7651.
6 A. S. Arico, V. Baglio, A. Di Blasi, V. Antonucci, L. Cirillo, A. Ghielmi and V. Arcella, *Desalination*, 2006, **199**, 271–273.
7 L. Merlo, A. Ghielmi, L. Cirillo, M. Gebert and V. Arcella, *Sep. Sci. Technol.*, 2007, **42**, 2891–2908.
8 J. Lin, Y. Liu and Q. M. Zhang, *Polymer*, 2011, **52**, 540–546.
9 K. D. Kreuer, M. Schuster, B. Obliers, O. Diat, U. Traub, A. Fuchs, U. Klock, S. J. Paddison and J. Maier, *J. Power Sources*, 2008, **178**, 499–509.
10 D. Gorri, M. G. De Angelis, M. Giacinti Baschetti and G. C. Sarti, *J. Membr. Sci.*, 2008, **322**, 383–391.
11 M. G. De Angelis, S. Lodge, M. Giacinti Baschetti, G. C. Sarti, F. Doghieri, A. Sanguineti and P. Fossati, *Desalination*, 2006, **193**, 398–404.
12 S. J. Paddison and J. Elliott, *ECS Trans.*, 2006, **1**, 207–214.
13 S. J. Paddison and J. A. Elliott, *Phys. Chem. Chem. Phys.*, 2006, **8**, 2193–2203.
14 J. Liu, N. Suraweera, D. J. Keffer, S. Cui and S. J. Paddison, *J. Phys. Chem. C*, 2010, **114**, 11279–11292.
15 D. Wu, S. J. Paddison and J. A. Elliott, *Macromolecules*, 2009, **42**, 3358–3367.
16 S. Ahadian, H. Mizuseki and Y. Kawazoe, *J. Membr. Sci.*, 2011, **369**, 339–349.
17 D. Brandell, J. Karo, A. Liivat and J. Thomas, *J. Mol. Model.*, 2007, **13**, 1039–1046.
18 I. H. Hristov, S. J. Paddison and R. Paul, *J. Phys. Chem. B*, 2008, **112**, 2937–2949.
19 R. B. Moore and C. R. Martin, *Macromolecules*, 1989, **22**, 3594–3599.
20 G. Gebel and R. B. Moore, *Macromolecules*, 2000, **33**, 4850–4855.
21 J. Peron, D. Edwards, M. Haldane, X. Y. Luo, Y. M. Zhang, S. Holdcroft and Z. Q. Shi, *J. Power Sources*, 2011, **196**, 179–181.
22 T. J. Peckham, J. Schmeisser, M. Rodgers and S. Holdcroft, *J. Mater. Chem.*, 2007, **17**, 3255–3268.
23 M. Adachi, T. Navessin, Z. Xie, B. Frisken and S. Holdcroft, *J. Electrochem. Soc.*, 2009, **156**, B782–B790.
24 C. Chuy, V. I. Basura, E. Simon, S. Holdcroft, J. Horsfall and K. V. Lovell, *J. Electrochem. Soc.*, 2000, **147**, 4453–4458.
25 V. Arcella, A. Ghielmi and G. Tommasi, *Ann. N. Y. Acad. Sci.*, 2003, **984**, 226–244.
26 Z. Shi and S. Holdcroft, *Macromolecules*, 2005, **38**, 4193–4201.
27 T. Astill, Z. Xie, Z. Q. Shi, T. Navessin and S. Holdcroft, *J. Electrochem. Soc.*, 2009, **156**, B499–B508.
28 V. I. Basura, P. D. Beattie and S. Holdcroft, *J. Electroanal. Chem.*, 1998, **458**, 1–5.

29 P. D. Beattie, V. I. Basura and S. Holdcroft, *J. Electroanal. Chem.*, 1999, **468**, 180–192.
30 Z. Xie and S. Holdcroft, *J. Electroanal. Chem.*, 2004, **568**, 247–260.
31 T. Biegler, D. A. J. Rand and R. Woods, *J. Electroanal. Chem.*, 1971, **29**, 269–277.
32 S. J. Paddison and J. A. Elliott, *J. Phys. Chem. A*, 2005, **109**, 7583–7593.
33 P. D. Beattie, V. I. Basura and S. Holdcroft, *J. Electroanal. Chem.*, 1999, **468**, 180–192.
34 V. I. Basura, C. Chuy, P. D. Beattie and S. Holdcroft, *J. Electroanal. Chem.*, 2001, **501**, 77–88.
35 G. Dorenbos and K. Morohoshi, *J. Chem. Phys.*, 2011, **134**, 44133.
36 J. Karo, A. Aabloo, J. O. Thomas and D. Brandell, *J. Phys. Chem. B*, 2010, **114**, 6056–6064.
37 G. Dorenbos and K. Morohoshi, *Energy Environ. Sci.*, 2010, **3**, 1326–1338.
38 G. Dorenbos and Y. Suga, *J. Membr. Sci.*, 2009, **330**, 5–20.

